PHYSICAL REVIEW A **80**, 021602(R) (2009)

Two-dimensional quantum gas in a hybrid surface trap

J. I. Gillen, W. S. Bakr, A. Peng, P. Unterwaditzer, S. Fölling, and M. Greiner
Department of Physics and Harvard-MIT Center for Ultracold Atoms, Harvard University, Cambridge, Massachusetts 02138, USA
(Received 16 December 2008; published 14 August 2009)

We demonstrate the realization of a two-dimensional (2D) quantum gas in a smooth optical surface trap. Using a combination of evanescent wave, standing wave, and magnetic potentials, we create a long-lived quantum gas deep in the 2D regime at a distance of a few microns from a glass surface. To realize a system suitable for many-body quantum simulation, we introduce methods such as broadband "white" light to create evanescent and standing waves to realize a smooth potential with a trap frequency aspect ratio of 300:1:1. We are able to detect phase fluctuations and vortices, and we demonstrate cooling to degeneracy and low disorder in the 2D configuration.

DOI: 10.1103/PhysRevA.80.021602 PACS number(s): 03.75.Lm, 67.85.Hj, 67.85.Jk

Ultracold quantum gases are increasingly used to experimentally realize and quantitatively study fundamental models of condensed-matter physics [1]. As many of the phases currently of interest such as *d*-wave superfluid states and antiferromagnets [2] appear in two dimensions, two-dimensional (2D) quantum gases [3–7] are of special relevance for carrying out "quantum simulations" of condensed-matter phenomena. In addition, some effects are unique to 2D systems such as the Berezinskii-Kosterlitz-Thouless (BKT) transition [8] recently observed in ultracold atoms [9–11]. 2D gases are characterized by a strong confinement in one direction with an energy scale much larger than that given by either the temperature or interparticle interactions.

The centerpiece of an experimental system for 2D quantum simulation is an atom trap that fulfills a number of criteria. The axial confinement of the trap must be very strong to be deep in the 2D regime even for large atom numbers, while the weak lateral confinement should be free of disorder. Additionally, it is desirable to have a trap configuration that enables the reliable preparation of a single plane of atoms to avoid averaging effects during state readout, as well as the preparation of dual planes for heterodyne phase measurements [6]. Finally, high aperture optical access to the quantum gas is desirable for probing and manipulation at small length scales.

Different approaches for reaching the 2D regime have been experimentally realized [1]. Repulsive evanescent wave (EW) potentials, originally introduced to reflect atoms from surfaces [12,13], were combined with gravity to form a gravito-optical surface trap [14,15]. In this trap a 2D Bose-Einstein condensate (BEC) was observed [5]. However, such traps have so far been limited by strong potential corrugations which led to inhomogeneous trap characteristics across the surface as well as inhibited expansion of the BEC [5,16]. The strongest axial confinement in 2D systems has been achieved in optical dipole standing-wave (SW) traps where a stack of 2D planes is populated by a BEC [6,7,17]. It is possible to empty all but a few planes by a radio-frequency "knife" [6] but precisely controlling the population remains a challenge, in particular for traps with strong confinement and small periodicity.

Here we demonstrate preparation of a 2D degenerate quantum gas close to a surface using a trapping scheme which overcomes limitations of current methods. It is designed to provide the confinement defined by requirements stated above while enabling maximal optical access. Our hybrid trapping potential is based on a dielectric surface used to combine an evanescent wave, nodal planes of reflected light and a magnetic confinement (Fig. 1). A surface trap approach provides us with several important advantages. Using a high quality dielectric surface as our reference, we are able to precisely and reproducibly overlap optical potentials. In contrast to free-space lattices the surface approach allows us to

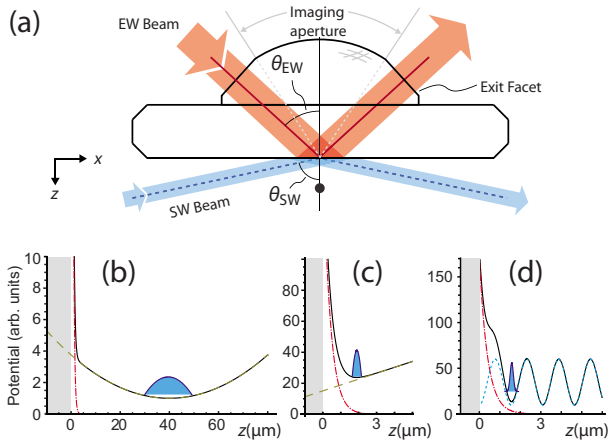

FIG. 1. (Color online) Hybrid trap. (a) The trap is based on a dielectric surface formed by the superpolished horizontal bottom face of a fused silica substrate. Fused to the top of the substrate is a hemispherical lens with lateral planar facets which is designed to be part of a high numerical aperture imaging system. Three potentials form the trap: an EW beam from the top generates an exponential repulsive potential (red dash-dotted lines). A beam reflected off the bottom side of the surface creates a standing wave (SW, blue dotted lines). A parabolic magnetic trap (green dashed lines) provides an upwards force and lateral confinement. (b) Schematic of magnetic trap potential with BEC closely below surface. The black line denotes the combined potential. (c) Evanescent wave configuration loaded by shifting the magnetic trap minimum inside the glass generating confinement between the magnetic gradient and the evanescent wave. (d) Atoms loaded into single plane of SW trap, 1.5 μm from the surface. The trap provides deep 2D confinement with lateral trap frequencies of $2\pi\times 20$ Hz and a vertical confinement of $2\pi\times 5.9$ kHz.

directly load all atoms into one or two planes. The proximity of these planes to the surface facilitates imaging them with high resolution due to a solid immersion effect [18]. This effect increases the geometric aperture NA=0.55 by a factor of n, the index of refraction, to higher effective NA=0.8, which allows for an imaging resolution of ≈0.5 micron. The vicinity of the gas to the surface also opens the door to precision studies of surface physics [19–21]. By using techniques such as "white" light broadband dipole potentials we are able to avoid potential corrugations. Long-lived coherent quantum gases deep in the 2D regime are obtained, and we are able to achieve low temperatures by evaporative cooling in the 2D trap. We observe long-wavelength phase fluctuations and, at higher temperatures, vortices, as expected from BKT physics.

The evanescent wave potential is created using blue-detuned light that is totally internally reflected at the interface of a dielectric medium and a vacuum [22]. The EW that appears on the vacuum side creates an exponentially decaying potential $V_{\mathrm{EW}}(z)=V_0\exp(-2z/\Lambda)$, where z is the distance to the surface, Λ is the decay length of the EW, and V_0 is the potential height at the surface given by the total incoming intensity.

Evanescent wave traps are particularly susceptible to disorder in the lateral potential. One very significant source of disorder is stray light that interferes with the trap light. This can cause sizable potential modulations at high spatial frequencies even for weak stray light intensities. We address this effect in multiple ways. First, we disable the interference between the trap light and most of the stray light from reflections, dust, and surface imperfections by using white light with a very short coherence length. The light is created by a two-stage tapered amplifier (TA) system, delivering 400 mW of light. The TAs are seeded with 6 mW of light from a fiber-coupled amplified spontaneous emission (ASE) source (superluminescent diode). Interference filters before and after the TAs are used to control the bandwidth of the white light source as well as to suppress resonant ASE components. The resulting approximately 3-nm-wide spectrum is centered on a wavelength of $\lambda_{trap}=765$ nm, with an incident power of 200 mW. We measure a coherence length of 160 ± 10 μm (50% decay path length difference), which is short enough to suppress the interference effects of stray light from multiple reflections in the glass substrate as well as most scatterers outside the radius given by the coherence length. A second measure employed for reducing inhomogeneities is the minimization of scatter at the trapping surface by using a superpolished and very clean surface with an rms surface roughness below 1 Å. This reduces corrugations due to scatter from locations within the range of the coherence length. We measured the residual scattered fraction at the glass vacuum interface to be less than 1 ppm.

Neutral atoms in close vicinity to surfaces can also be affected by static electric potentials. Adsorbed metal atoms on the surface form small electric dipoles. Inhomogeneities of the distribution of these dipoles generate potential gradients which can be stronger than the inherent van der Waals force of the substrate. This process is well understood [23,24] and the fields generated decay very rapidly away from the surface. By minimizing Rb deposition on the glass, detrimental effects are avoided at a moderate distance $d=1.5$ μm from the surface.

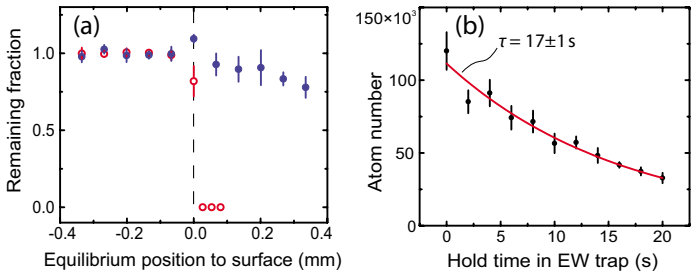

FIG. 2. (Color online) (a) Moving the atoms against the surface without EW leads to a sudden loss (red circles), which is avoided by the repulsive potential (blue filled circles). (b) Atom lifetime in the hybrid EW trap, red line corresponds to fit with single exponential.

Our experiments start with a three-dimensional (3D) BEC of several 10^5 ^{87}Rb atoms. The BEC is created by loading a magneto-optic trap for 8 s, resulting in 10^9 atoms at a temperature of 40 μK after optical molasses cooling. We then magnetically transport [25] the atoms into a glass cell with very good vacuum ($\approx 2\times10^{-11}$ mbar)[25], inside which the substrate is mounted. Here, we perform forced rf evaporation in a tightly confining quadrupole-Ioffe configuration (QUIC) trap [26] with frequencies of $\omega_{x,y,z}=2\pi(17,100,100)$ Hz to achieve BEC. Following this, we change to a high (102 G) offset field configuration with reduced trap frequencies of $2\pi(17,20,20)$ Hz. At this stage, the BEC is 0.6 mm below the surface.

The evanescent wave trap configuration is formed by moving the magnetic trap vertically upwards using external magnetic fields. The equilibrium position is moved by 1.6 mm, well beyond the fused silica surface. When it passes the surface, the atoms are vertically held in place by the EW, giving rise to a combined optomagnetic surface trap [Fig. 2(a)]. The EW beam is an elliptic beam of 250 μm $\times$ 180 μm size incident at an angle θ_{EW}, 12 mrad from the critical angle θ_c (Fig. 1). The decay length Λ is given by $(\lambda_{trap}/2\pi)/[n^2\sin^2(\theta_{\mathrm{EW}})-1]^{1/2}\approx 800$ nm where n is the index of refraction of fused silica. The overall potential is repulsive up to a maximum at a distance of ≈200 nm from the surface, below which the attractive van der Waals potential dominates. The short decay length of the EW gives rise to large curvatures that allow tight confinement along the direction of the decay. Trap frequencies of up to $2\pi\times1$ kHz measured by parametric excitation can be reached in this configuration. In this 2D configuration, we observe a $1/e$ atom lifetime τ of 17 ± 1 s [Fig. 2(b)]. To verify the lateral homogeneity of the resulting potential, we dynamically transport the cloud over the diameter of the EW beam (by displacing the magnetic field center up to 250 μm) without causing significant heating or atom loss due to "holes" in the evanescent wave.

To further increase the vertical confinement and improve the lateral homogeneity, we use an additional standing-wave potential. The larger trap frequencies allow us to reach the deep 2D regime for higher atom numbers as well as to achieve stronger interactions in the system. The standing-wave potential is generated by reflecting a blue-detuned

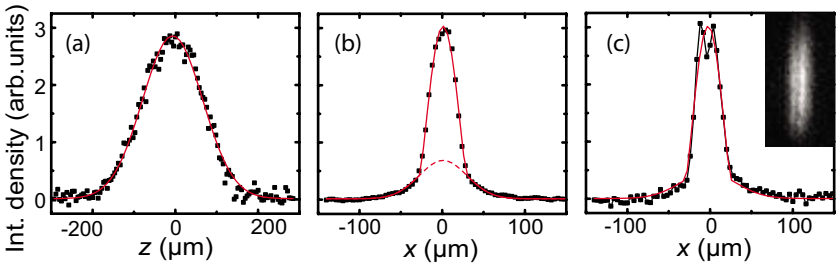

FIG. 3. (Color online) Quantum gas deep in 2D regime. Time of flight images from standing wave trap: (a) the vertical density profile is Gaussian, showing that the system is deep in the 2D configuration. In the lateral direction, it is well described by a bimodal Thomas-Fermi profile with ≈20% thermal fraction in this case: (b) integrated lateral profile averaged over 86 samples and (c) density fluctuations caused by thermal 2D phase fluctuations in single profile from same data set (inset shows 140 μm × 280 μm).

beam off the glass surface from the vacuum side [27]. Incident at an angle $\theta_{SW}=75°$ from the normal, the trap minima in the resulting potential are planes parallel to the surface with a spacing of ≈1.5 μm. Compared to the evanescent wave trap the trap frequency is increased by a factor of more than 5. Contrary to all current standing wave traps, the potential is formed not by coherent light but by light from the 765 nm broadband source. This reduces disorder from stray light interference but does not significantly affect the interference contrast as the coherence length of the light is still much larger than the interfering distance $2d \cos \theta_{SW}$.

The SW configuration also reduces further the disorder caused by the remaining scattered light interference from those parts of the glass which are closer than the coherence length. As the SW has an intensity minimum at the surface as opposed to the intensity maximum of the EW, scattering from small surface impurities is suppressed.

We reliably load all of the atoms into a single node of the standing wave, as the spread of the wave function (z_{ho} =250 nm) in the pure EW trap is much smaller than the spacing of the SW planes. The transfer is realized by smoothly shifting power from the EW beam to the standing-wave beam over a period of 300 ms. The trap frequency in the z direction verified by parametric excitation measurements is increased to 5.9 ± 0.1 kHz in this trap, taking us deep into the 2D regime with the temperature and chemical potential both much smaller than the vertical trap frequency [4]. We populate the first node of the SW at a distance of ≈1.5 μm from the surface. At this distance, the disorder caused by small amounts of surface dipoles is already strongly reduced, and the distance from the surface is small enough to exploit the NA enhancement when imaging through the substrate. In order to confirm the lateral homogeneity of the potential we move a bimodal ensemble 200 μm back and forth across the surface within 150 ms. We do not observe any heating ($\Delta T=-4.3$ nK ± 4.0 nK) or atom loss ($\Delta N/N=3.4 \pm 2.4$ %) during this process. Another indication for the smoothness of the potential is that the atoms are free to leave it by moving out of the beam within a few 10 ms when switching off the magnetic potential due to a weak remaining anticonfinement.

The 2D regime manifests itself as a change in the shape of the momentum distribution measured in time of flight along the z direction. We obtain a Gaussian momentum profile along the vertical [Fig. 3(a)] corresponding to the harmonic confinement of the trap, while the profile along the other direction remains Thomas-Fermi [Fig. 3(b)]. The 2D system with $\approx 2 \times 10^4$ atoms is below the expected BKT transition temperature of $T_{BKT} \approx 40$ nK at which vortices proliferate in the condensate [1]. Below T_{BKT}, phase fluctuations in the condensate fraction can be present which are mapped to density fluctuations [28] in time of flight as seen in Fig. 3(c). These fluctuations decrease with the temperature of the condensate during the second evaporation step. The SW configuration allows us to perform forced rf evaporation inside the 2D trap using a radial magnetic field gradient to evaporate along the outer edge of the trap volume. By stabilizing the current for the bias magnetic field of the QUIC trap to ~3 ppm, we obtain a stable evaporation process with reproducible atom numbers in the desired range of several 10^4 atoms.

The $1/e$ lifetime in the SW trap is 7.8 ± 0.4 s, and we have used both the incoherent light and a narrow band 765 nm cw Ti:sapphire laser for comparison. We find the lifetimes to be the same within the error of the measurements and consistent with loss due to spontaneous emission, indicating that there are no additional loss/heating processes (e.g., photo-association) associated with using the broadband light source.

We can also intentionally load two planes of the SW trap by weakening the confinement and choosing a larger separation from the surface in the initial EW configuration. When two planes are loaded, a vertical sinusoidal interference pattern appears after ballistic time of flight (Fig. 4), which can be used to detect long-range phase fluctuations and vortices in the trap [6]. In order to quantitatively probe the distribution over the trap nodes, we employ rf spectroscopy similar to that done in [6], using a magnetic field gradient of 33.8 ± 0.7 G/cm perpendicular to the surface. The density distribution along the gradient direction is then probed by varying the rf according to a scaling of 2.43 ± 0.05 kHz/ μm. This achieves a spatial resolution better than 1 μm. The vertical potential periodicity is 1.54 ± 0.04 μm determined by diffracting atoms off the SW. The profile is shown in Fig. 4(d) using an rf pulse length of 2 s. The two loaded sites can be clearly distinguished. Conversely, when loading a single site, the profiling yields an upper limit for the occupation in the second site of ≈5%, while the (lack of) interference during ballistic expansion limits the fraction of the total coherent population in that site to less than $\approx 10^{-3}$.

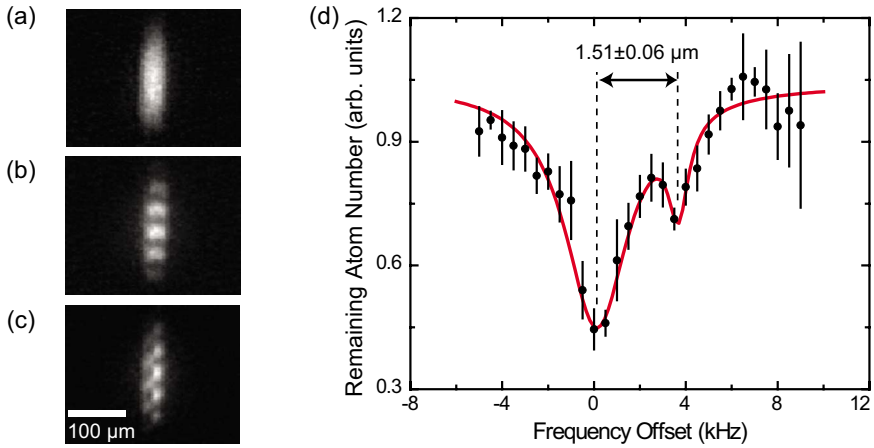

FIG. 4. (Color online) Loading of single and multiple planes in the standing-wave trap. (a) atoms loaded into a single site, imaged from the side after release and 17 ms time-of-flight, and (b) interference between atoms from two planes. (c) Interference pattern between two planes at a higher temperature showing the presence of a thermally activated vortex. (d) The vertical density profile obtained by rf addressing shows the occupation of two planes. The red line denotes a two-peak Lorentzian fit, which yields a peak separation of 1.51 ± 0.06 μm.

In conclusion, we demonstrate a scheme of creating a quantum gas deep in the 2D regime close to a glass surface. The trap provides both strong confinement in the vertical direction and smooth potentials in the 2D plane without the necessity to load many planes simultaneously. We avoid interference of scattered light with the trap light by employing light sources which have short coherence lengths. We create 2D quantum gases and are able to detect properties such as phase fluctuations and thermal excitation of vortices. By making the trapping surface a part of a microscope, we achieve a very high aperture optical access that enables a resolution of 500 nm (rms) for imaging, creating optical potentials, and manipulating atoms. These capabilities enable a wide range of experiments, including optical lattices that combine single-site resolution and strong tunnel coupling in the ground state and experiments on phase fluctuations and vortices in 2D quantum gases.

Note added. Recently, we learned of work describing another approach of combining magnetic and EW potentials designed for quantum optics [29].

We thank H. Brachmann for contributions during the construction of the experiment. We acknowledge support from NSF, AFOSR, DARPA, and Sloan. J.I.G. and S.F. acknowledge additional support from the NSF and IQSE, respectively.

[1] I. Bloch, J. Dalibard, and W. Zwerger, Rev. Mod. Phys. **80**, 885 (2008).
[2] P. A. Lee, N. Nagaosa, and X.-G. Wen, Rev. Mod. Phys. **78**, 17 (2006).
[3] N. L. Smith *et al.*, J. Phys. B **38**, 223 (2005).
[4] A. Görlitz *et al.*, Phys. Rev. Lett. **87**, 130402 (2001).
[5] D. Rychtarik, B. Engeser, H. C. Nägerl, and R. Grimm, Phys. Rev. Lett. **92**, 173003 (2004).
[6] S. Stock *et al.*, Phys. Rev. Lett. **95**, 190403 (2005).
[7] M. Köhl *et al.*, J. Low Temp. Phys. **138**, 635 (2005).
[8] J. Kosterlitz and D. Thouless, J. Phys. C **6**, 1181 (1973).
[9] Z. Hadzibabic *et al.*, Nature (London) **441**, 1118 (2006).
[10] V. Schweikhard, S. Tung, and E. A. Cornell, Phys. Rev. Lett. **99**, 030401 (2007).
[11] P. Cladé, C. Ryu, A. Ramanathan, K. Helmerson, and W. D. Phillips, Phys. Rev. Lett. **102**, 170401 (2009).
[12] V. I. Balykin, V. S. Letokhov, Y. B. Ovchinnikov, and A. I. Sidorov, Phys. Rev. Lett. **60**, 2137 (1988).
[13] A. Landragin *et al.*, Opt. Lett. **21**, 1591 (1996).
[14] Y. B. Ovchinnikov, I. Manek, and R. Grimm, Phys. Rev. Lett. **79**, 2225 (1997).
[15] M. Hammes, D. Rychtarik, B. Engeser, H. C. Nägerl, and R. Grimm, Phys. Rev. Lett. **90**, 173001 (2003).
[16] D. Rychtarik, Ph.D. thesis, Universität Innsbruck, 2004.
[17] I. B. Spielman, W. D. Phillips, and J. V. Porto, Phys. Rev. Lett. **98**, 080404 (2007).
[18] S. M. Mansfield and G. S. Kino, Appl. Phys. Lett. **57**, 2615 (1990).
[19] A. Landragin *et al.*, Phys. Rev. Lett. **77**, 1464 (1996).
[20] Y.-J. Lin, I. Teper, C. Chin, and V. Vuletic, Phys. Rev. Lett. **92**, 050404 (2004).
[21] D. M. Harber, J. M. Obrecht, J. M. McGuirk, and E. A. Cornell, Phys. Rev. A **72**, 033610 (2005).
[22] R. Grimm, M. Weidemüller, and Y. B. Ovchinnikov, Adv. At., Mol., Opt. Phys. **42**, 95 (2000).
[23] J. M. McGuirk, D. M. Harber, J. M. Obrecht, and E. A. Cornell, Phys. Rev. A **69**, 062905 (2004).
[24] J. M. Obrecht, R. J. Wild, and E. A. Cornell, Phys. Rev. A **75**, 062903 (2007).
[25] M. Greiner, I. Bloch, T. W. Hänsch, and T. Esslinger, Phys. Rev. A **63**, 031401(R) (2001).
[26] T. Esslinger, I. Bloch, and T. W. Hänsch, Phys. Rev. A **58**, R2664 (1998).
[27] B. Engeser, Ph.D. thesis, Universität Innsbruck, 2006.
[28] S. Dettmer *et al.*, Phys. Rev. Lett. **87**, 160406 (2001).
[29] H. Bender, P. Courteille, C. Zimmermann, and S. Slama, Appl. Phys. B **96**, 275 (2009).